

# The effect of a biochar temperature series on denitrification: which biochar properties matter?



Simon Weldon<sup>a,c,\*</sup>, Daniel P. Rasse<sup>a</sup>, Alice Budai<sup>a</sup>, Oliver Tomic<sup>b</sup>, Peter Dörsch<sup>c</sup>

<sup>a</sup> Department of Soil Quality and Climate Change, Norwegian Institute of Bioeconomy Research, NIBO, Ås, Norway

<sup>b</sup> Faculty of Science and Technology, Norwegian University of Life Sciences, NMBU, Ås, Norway

<sup>c</sup> Faculty of Environmental Sciences and Natural Resource Management, Norwegian University of Life Sciences, NMBU, Ås, Norway

## ARTICLE INFO

### Keywords:

Biochar  
N<sub>2</sub>O  
NO  
Denitrification  
GHG mitigation  
Biochar properties

## ABSTRACT

Biochar has been shown to reduce nitrous oxide (N<sub>2</sub>O) emissions from soils, but the effect is highly variable across studies and the mechanisms are under debate. To improve our mechanistic understanding of biochar effects on N<sub>2</sub>O emission, we monitored kinetics of NO, N<sub>2</sub>O and N<sub>2</sub> accumulation in anoxic slurries of a peat and a mineral soil, spiked with nitrate and amended with feedstock dried at 105 °C and biochar produced at 372, 416, 562 and 796 °C at five different doses. Both soils accumulated consistently less N<sub>2</sub>O and NO in the presence of high-temperature chars (BC562 and BC796), which stimulated reduction of denitrification intermediates to N<sub>2</sub>, particularly in the acid peat. This effect appeared to be strongly linked to the degree of biochar carbonisation as predicted by the H:C ratio of the char. In addition, biochar surface area and pH were identified as important factors, whereas ash content and CEC played a minor role. At low pyrolysis temperature, the biochar effect was soil dependent, suppressing N<sub>2</sub>O accumulation in the mineral soil, but enhancing it in the peat soil. This contrast was likely due to the labile carbon content of low temperature chars, which contributed to immobilise N in the mineral soil, but stimulated denitrification and N<sub>2</sub>O emission in the peat soil. We conclude that biochar with a high degree of carbonisation, high pH and high surface area is best suited to suppress N<sub>2</sub>O emission from denitrification, while low temperature chars risk supporting incomplete denitrification.

## 1. Introduction

Biochar has a significant potential to mitigate greenhouse gas emissions from agriculture, both by storing carbon in soils (Lehmann et al., 2006; Lorenz and Lal, 2014) and through mitigating N<sub>2</sub>O emissions (Cayuela et al., 2014; He et al., 2017; Grutzmacher et al., 2018). In a recent meta-analysis, Borchard et al. (2019) reported an average reduction of N<sub>2</sub>O emission by biochar of 38 percent. This is a notable reduction in the estimated effect strength of 54 percent from a previous meta-analysis (Cayuela et al., 2014) and highlights the variability in biochar effects on N<sub>2</sub>O emissions from study to study. Some studies do not find any effect (Zheng et al., 2012; Wang et al., 2013; Case et al., 2014; Van Zwieten et al., 2014) while others report stimulation of N<sub>2</sub>O emissions (Yanai et al., 2007; Clough et al., 2010; Shen et al., 2014). Despite a significant body of research on the N<sub>2</sub>O suppressing effect of biochar, it is still not possible to predict whether the addition of a specific biochar will have a measurable effect on soil N<sub>2</sub>O emissions for a given combination of soil type, biochar feedstock, production method and dose. Variable effects may be expected, given the fact that N<sub>2</sub>O is

produced by a number of abiotic and biotic reactions in soil, with microbial nitrification and denitrification considered to be the most significant ones (Firestone and Davidson, 1989). Both processes respond differently to changes in abiotic factors brought about by biochar in soil, and it is unlikely that the N<sub>2</sub>O suppressing effect is governed by any singular property of the biochar. Here, we focus on denitrification and study in detail how biochar influences the microbial turnover of NO and N<sub>2</sub>O under anaerobic conditions.

Many studies examining the N<sub>2</sub>O suppressing effect of biochar have focused on N<sub>2</sub>O emissions (Jia et al., 2012; Fungo et al., 2014; Verhoeven and Six, 2014; Edwards et al., 2018), while relatively few have addressed underlying processes (Ameloot et al., 2013; Cornelissen et al., 2013; Nelissen et al., 2014; Obia et al., 2015; Harter et al., 2017; Chen et al., 2018). Among the latter, studies addressing the enzymatic reduction of N<sub>2</sub>O to N<sub>2</sub> in denitrification are of particular interest. Biochar has been implicated to act directly as a redox mediator supporting the reduction of N<sub>2</sub>O to N<sub>2</sub> in denitrification (Cayuela et al., 2013) or by changing the denitrifying community composition to be more efficient in reducing N<sub>2</sub>O (Van Zwieten et al., 2014; Harter et al.,

\* Corresponding author. Department of Soil Quality and Climate Change, Norwegian Institute of Bioeconomy Research, NIBO, Ås, Norway.

E-mail address: [simon.weldon@nibio.no](mailto:simon.weldon@nibio.no) (S. Weldon).

2017). Others have highlighted the alkalizing effect of biochar in acid soils as a possible explanation for increased microbial N<sub>2</sub>O reduction in acidic soils (Obia et al., 2015; Harter et al., 2016).

Providing evidence for complete denitrification in soil is not trivial, because quantification of N<sub>2</sub> production requires sophisticated incubation setups or stable isotope approaches. Recent studies have inferred the functioning of denitrification from copy numbers of key denitrification gene transcripts (Xu et al., 2012; Harter et al., 2017), documenting increased ratios of *nosZ* (coding for N<sub>2</sub>O reductase) over *nirK* and/or *nirS* transcripts (coding for NO<sub>2</sub><sup>−</sup> reductase), which was taken as evidence for biochar promoting N<sub>2</sub>O reducing microorganisms. However, primer-based studies into the composition of actively denitrifying communities may be biased (Roco et al., 2017) and biochar mediated changes in the taxonomic composition of denitrifier communities require time to manifest (Brenzinger et al., 2015). By contrast, monitoring of the gaseous denitrification products can quantify direct effects of biochar on N<sub>2</sub>O turnover by denitrification and provide valuable information about the stoichiometry of denitrification products (Cayuela et al., 2013; Obia et al., 2015; Chen et al., 2018).

Nitric oxide (NO), the precursor of N<sub>2</sub>O in denitrification, is rarely studied in the context of biochar research (Nelissen et al., 2014; Obia et al., 2015). NO is a significant atmospheric pollutant (Molina-Herrera et al., 2017; Pourhashem et al., 2017), but also an important signalling molecule during the early induction of denitrification (Nadeem et al., 2013). Therefore, studying denitrification kinetics, i.e. the sequential production and consumption of NO and N<sub>2</sub>O and the accumulation of the final product N<sub>2</sub> in the presence and absence of biochar may shed light on the underlying biochar-driven mechanisms suppressing denitrification-induced N<sub>2</sub>O production.

Biochars comprise a wide array of structural and chemical properties, all of which may affect the redox reactions involved in denitrification. The physico-chemical properties of biochar are a function of feedstock type, pyrolysis method and pyrolysis temperature (Antal and Gronli, 2003; Kloss et al., 2012). Increasing pyrolysis temperature decreases volatile matter and increases the relative content of C to O and H in biochar. Indices such as a H:C ratio of < 0.3 of biochar have been suggested as proxies for N<sub>2</sub>O suppressing properties (Cayuela et al., 2015), but little is known about the actual properties responsible or their modes of action. Increasing pyrolysis temperature also increases ash content and aromaticity, while surface area and surface functionality, i.e. the capacity to donate and receive electrons, increase non-linearly with pyrolysis temperature (Budai et al., 2014; Klüpfel et al., 2014a). This suggests that thresholds in pyrolysis temperature with respect to N<sub>2</sub>O suppression may exist.

Biochar properties may affect denitrification in various ways; through sorption or desorption of NO<sub>2</sub><sup>−</sup> or NO<sub>3</sub><sup>−</sup> (Yao et al., 2012; Hagemann et al., 2017), DOC (Lu et al., 2014) and gaseous intermediates (Cornelissen et al., 2013), through increasing the activity and/or completeness of denitrification by pH increase (Wijler and Delwiche, 1954; Bakken et al., 2012) or by redox mediation (Cayuela et al., 2013; Klüpfel et al., 2014a; Chen et al., 2018). However, the effects may be antagonistic, as more complete denitrification may go along with increased denitrification, thus potentially nulling out N<sub>2</sub>O suppression.

The present study focuses on the effect of biochar on NO and N<sub>2</sub>O turnover in denitrification under controlled conditions, with biochar treatment temperature, dose and soil type being the main variables. We used batch incubations of constantly stirred soil slurries in a helium atmosphere to minimize matrix effects and monitored the accumulation of gaseous denitrification products (N<sub>2</sub>, N<sub>2</sub>O, NO, CO<sub>2</sub>) at high temporal resolution. Our objective was to elucidate how the N<sub>2</sub>O suppressive effect of a corncob biochar, in two contrasting soils (a mineral soil and a peat), depends on its physico-chemical properties as affected by highest treatment temperature during pyrolysis.

**Table 1**

Key soil properties. (Mean and Standard deviation n = 3).

	Peat		Mineral soil	
pH <sub>(H2O)</sub>	5.08	( ± 0.00)	5.86	( ± 0.04)
C %	53.00	( ± 0.10)	2.83	( ± 0.01)
N %	1.79	( ± 0.04)	0.29	( ± 0.00)
C:N	29.53	( ± 0.70)	9.87	( ± 0.21)
H <sup>+</sup> (mmol/kg)	689.73	( ± 9.43)	93.27	( ± 0.90)
Ca (mmol/kg)	314.40	( ± 5.06)	44.69	( ± 0.68)
K (mmol/kg)	7.91	( ± 0.17)	2.80	( ± 0.03)
Mg (mmol/kg)	68.35	( ± 0.98)	2.34	( ± 0.03)
Mn (mmol/kg)	0.09	( ± 0.00)	0.11	( ± 0.00)
Na (mmol/kg)	16.75	( ± 0.14)	0.75	( ± 0.01)
CEC (cmol/kg)	1480.10	( ± 21.04)	191.08	( ± 2.35)
Base saturation (%)	53.38	( ± 0.20)	51.07	( ± 0.16)

## 2. Materials and methods

### 2.1. Biochars and soils

Samples of top-soils (0–10 cm) were collected from a cultivated peatland and an acid mineral soil, classified as Hemic Histosol and Umbric Epistagnic Albeluvisol (WRB), respectively. Soils were stored at 4 °C until experimentation and sieved to 2 mm before incubation. Table 1 gives key properties of the soils.

A series of biochars was prepared from *Zea mays* corncobs using slow pyrolysis in N<sub>2</sub> atmosphere. Methods of preparation and storage are given in Budai et al. (2014). In brief, a heating rate of 2.5 °C min<sup>−1</sup> was used, and highest treatment temperatures (HTT) were measured within the 1 L retort. HTTs of samples selected for this study were 105, 372, 416, 562 and 769 °C, hereafter referred to as FS105, BC372, BC416, BC562 and BC796. The sequence was chosen to span a wide range of biochar key properties such as pH, CEC, volatile matter (VM) and ash content. The biochars were crushed through a 2 mm sieve and stored dry.

Table 2 lists the biochar properties. pH<sub>(H2O)</sub> ranged from 8.8 to 10.1 and ash content from 2.1 to 4.5% w/w. Volatile matter content ranged from 6.9 to 40.5% and the C content from 71.9 to 91.5% w/w. Less than 0.1% w/w was readily biodegradable in soil regardless of pyrolysis temperature, as determined in a one-year incubation study (Budai et al., 2016). The yearly mineralization rate of the remaining C pool of the biochars was approximately 0.005 y<sup>−1</sup>. Where possible, variables were scaled to the biochar dose added. Where this was not possible, e.g. for elemental ratios, properties are given as single value.

### 2.2. Experimental design

Denitrification kinetics were studied in two separate incubation experiments, one with each soil type. Each soil was incubated with multiple combinations of HTT and dose, each unique combination being represented by one incubation flask on which time-repeated measures were carried out to determine denitrification kinetics and derive denitrification parameters. Non-amended soils were incubated in triplicate to judge the extent of variability in N gas kinetics in our experimental set up. The statistical power of the experiment resides in the controlled nature of our incubations (see ch. 2.3) which typically guarantees high reproducibility between replicates (e.g. Obia et al., 2015). Soils were homogenised and incubated as constantly stirred, temperature controlled slurries to reduce matrix effects and ensure homogeneity. Oxygen was removed effectively (data not shown) by repeated evacuation and He-washing prior to each experiment, creating a highly controlled experimental system for testing the effect of incremental biochar HTTs and doses in two contrasting soils. This design was chosen to focus on relative changes in denitrification responses induced by linear changes in biochar properties. Our cross-validated partial least squares regression (PLSR) model confirmed that there was a high

**Table 2**

Key properties of corn cob biochars used in this study. HTT - highest temperature treatment; BPCA:C - benzene polycarboxylic acid to carbon ratio, an indicator of aromaticity; B6CA:C - benzenehexacarboxylic acid to C ratio, an indicator of condensation; aliCH:aroCH - ratio of aliphatic to aromatic CHs measured by MIR; H:C, O:C - Elemental ratios; VM - Volatile matter; fC - Fraction of fixed carbon; Ash - Ash fraction; CEC - Cation exchange capacity; SA - Surface area. All data from [Budai et al. \(2014\)](#). See [Table 3](#) for methods of determination.

HTT	BPCA:C	B6CA:C	aliCH:aroCH	H:C	O:C	N:C	VM	fC	Ash	pH	CEC	SA
°C	ratio			Molar ratio			%	%	%		cmol/kg	m <sup>2</sup> /g
105	18.34	0.00	4.52	1.62	0.89	0.0066	81.08	17.47	1.45	5.34	14.88	1.82
372	122.16	32.76	1.56	0.80	0.27	0.0061	40.46	57.42	2.12	8.84	14.86	1.26
416	164.16	45.01	0.75	0.59	0.17	0.0056	26.38	70.46	3.16	10.07	16.21	3.58
562	167.45	61.36	0.22	0.37	0.08	0.0083	12.66	83.94	3.40	9.36	13.46	44.93
796	192.58	136.02	0.23	0.13	0.04	0.0096	6.88	88.67	4.46	9.44	5.07	27.44

degree of predictability in denitrification response by both dose and biochar HTT.

### 2.3. Denitrification kinetics

Soil-biochar mixtures were incubated as continuously stirred anoxic slurries in 120 ml serum flasks. Slurries were chosen to ensure full mixing of biochars with the soil, to minimize diffusional constraints and to aid equilibration of gases between the liquid and the gaseous phase (i.e. headspace of the flasks). After washing the slurries with helium, headspace concentrations of O<sub>2</sub>, N<sub>2</sub>, N<sub>2</sub>O, NO and CO<sub>2</sub> were measured every 5 h for 182–235 h in the peat and mineral soil, respectively, using a fully automated, temperature controlled incubation system similar to that described by [Molstad et al. \(2007\)](#) with modifications documented in [Molstad et al. \(2016\)](#). We varied the length of the incubations with the aim of allowing time for treatments with lower denitrification rates to achieve complete denitrification of soil native and added NO<sub>3</sub><sup>−</sup>, as indicated by a plateau in N<sub>2</sub> accumulation.

The flasks were incubated in a temperature controlled water bath holding 30 flasks, continuously stirred by submersible magnetic stirrers in a water bath. The flasks were sampled every 5 h by a hypodermic needle operated by an auto-sampler (CTC PAL). For each sampling, ~1 ml of headspace gas is pumped to dedicated sampling loops of a gas chromatograph (Model 7890A, Agilent, Santa Clara, CA, USA) using a programmable peristaltic pump (Gilson minipuls3) with Marprent tubing. The GC is equipped with a 30 m PoraPLOT-U column operated at 36 °C for separating N<sub>2</sub>O, CH<sub>4</sub> and CO<sub>2</sub> from bulk gases and a 30 m 5 Å Molsieve column operated at 50 °C for separating N<sub>2</sub> and O<sub>2</sub>. Low concentrations of N<sub>2</sub>O were quantified by an electron capture detector operated at 340 °C using ArCH<sub>4</sub> (90/10 vol%) as make up gas. CO<sub>2</sub>, O<sub>2</sub>, N<sub>2</sub> and high mixing ratios of N<sub>2</sub>O were quantified by a thermal conductivity detector. Nitric oxide (NO) concentrations were measured by a chemoluminescence NO<sub>x</sub>-analyzer (Model 200A, Advanced Pollution Instrumentation, San Diego, CA) coupled inline to one of the sampling loops of the GC. Headspace pressure was kept constant at ~1 atm by automatically reversing the pump after sampling and backfilling with helium. Multiple internal standard gases were included. He-dilution and O<sub>2</sub>/N<sub>2</sub> leakage were evaluated in blank flasks and used to correct the gas kinetics as described by [Molstad et al. \(2007\)](#). Based on the observation that there was a significant early accumulation in N<sub>2</sub> in our flasks, an additional abiotic experiment with stirred biochar suspensions was performed to assess desorption kinetics of residual N<sub>2</sub> into the He-atmosphere of the headspace as a function of biochar HTT and dose. This experiment is described in detail in the supplementary information (SI Section 1). Dissolution of gas and modelled desorption of N<sub>2</sub> after helium-washing were modelled and subtracted from the measured N<sub>2</sub> accumulation (for details see SI Section 1).

### 2.4. Treatments

Soil equivalent to 1.5 g dry weight of peat and 2 g dry weight of

mineral soil was weighed into 120 ml serum flasks equipped with magnetic stirrers. Biochar was added at increasing rates of 1, 5, 10, and 20% w/w. For the peat soil an additional treatment 30% w/w was set up because we expected that the BC effect might be masked at low doses in the carbon rich peat. After adding 30 ml of MilliQ water, the flasks were sealed with butyl rubber septa and made anoxic by repeated evacuation and He-filling (six times), while continuously stirring the slurries. 10 ml of degassed 4 mM KNO<sub>3</sub><sup>−</sup> solution was added, resulting in a final concentration of 1 mM KNO<sub>3</sub><sup>−</sup> (40 μmol N flask<sup>−1</sup>). All flasks were He-washed for an additional cycle before placing them in the water bath of the incubation system which was set to 15 °C. We chose this incubation temperature as it is closer to actual soil temperature in the temperate region than room temperature. After 10 min temperature equilibration, excess He was released. Headspace gases (CO<sub>2</sub>, O<sub>2</sub>, NO, N<sub>2</sub>O and N<sub>2</sub>) were monitored every 5 h until N<sub>2</sub> accumulation levelled off, indicating complete conversion of NO<sub>3</sub><sup>−</sup> to N<sub>2</sub>. After termination of the incubation, the flasks were opened and slurry pH and residual NO<sub>3</sub><sup>−</sup> and NO<sub>2</sub><sup>−</sup> (in the mineral soil only) were measured (SI section 2), before drying the slurries to determine dry weight soil in each bottle.

### 2.5. Data analysis

Measured denitrification kinetics ([Fig. S4 a, b](#)) were used to calculate a number of denitrification indices ([Table 3, Fig. 1](#)), including the N<sub>2</sub>O product ratio, N<sub>2</sub>O/(N<sub>2</sub> + N<sub>2</sub>O), calculated as a ratio of the integrated area under the curves for N<sub>2</sub>O and N<sub>2</sub>O + N<sub>2</sub> ([Liu et al., 2010](#)). We refer to this index as the Integrated Product Ratio (IPR). Since the amount of total N denitrified throughout the incubation differed between treatments, a cutoff had to be defined for calculating IPR. To account for differences in denitrification activity between the soils, the cut off for the peat was chosen at 20 μmol denitrified N, whereas the cut off for the mineral soil, which was less active, was chosen at 5 μmol denitrified N. The cut offs were chosen based on the lowest return of total μmol N denitrified among all treatments of each soil type throughout the full length of the incubation. Setting our limit in terms of μmol N denitrified, and not time, allowed us to normalise the treatments and to provide a more accurate comparison between treatments within each soil type. Other indices used were maximum denitrification (DR<sub>max</sub>) calculated as the maximum rate of NO + N<sub>2</sub>O + N<sub>2</sub> accumulation and the time needed since onset of anoxic incubation to obtain this maximum rate (T<sub>DRmax</sub>), as well as the maximum NO, N<sub>2</sub>O and N<sub>2</sub> concentrations reached during incubation, referred to as NO<sub>max</sub>, N<sub>2</sub>O<sub>max</sub> and N<sub>2max</sub>, respectively.

### 2.6. Statistical analyses

In order to examine the relationship between the indices of denitrification and biochar properties, we used PLSR ([Martens, 1987](#)). This method is not sensitive to issues of collinearity or autocorrelation and avoids arbitrary variable selection. We chose to use the biochar

**Table 3**  
Data structure for the PLSR model including descriptions of abbreviations and analysis methods.

Data Block <sup>a</sup>	Variable	Units	Description	Analysis method
X01	NO <sub>max</sub>	μmol N g dw <sup>-1</sup>	Maximum measured N2O or NO-N accumulation	GC incubation
X02	N <sub>2</sub> O <sub>max</sub>	μmol N g dw <sup>-1</sup>		
X03	N <sub>2</sub> max	μmol N g dw <sup>-1</sup>		
X04	IPR <sup>1</sup>	Ratio		
X05	NO:N <sub>2</sub> O		Integrated Product Ratio. This is the N <sub>2</sub> O product ratio [N <sub>2</sub> O/(N <sub>2</sub> O + N <sub>2</sub> )] calculated using the integral of each curve.	
X06	DR <sub>max</sub>	μmol N g dw <sup>-1</sup> hr <sup>-1</sup>	This is the ratio of NO to N <sub>2</sub> O calculated using the integral of each curve. This is the maximum rate measured for the total N curve.	
X07	T <sub>0.9</sub> max	hr	This is the time at which the maximum rate was achieved	
Y01	VM <sup>1</sup>	g flask <sup>-1</sup>	Volatile matter - ASTM method D 1762-84	ASTM method D 1762-84
Y02	Ash <sup>1</sup>	g flask <sup>-1</sup>	Ash content - ASTM method D 1102	ASTM method D 1102
Y03	fc <sup>1</sup>	%	Fixed carbon calculated by difference between 100% and the sum of measured VM and ash contents: %fc <sub>ash-free</sub> = 100 × $\frac{\%fc}{\%fc + \%vm}$	derived from VM and Ash content
Y04	SA <sup>1</sup>	m <sup>2</sup> flask <sup>-1</sup>	Surface area - measured using	Brunauer–Emmett–Teller method modified ammonium acetate compulsory displacement method derived from a 2 pool model fitted to an oxalic incubation Leco CHN1000 analyzer and coal reference material TruSpec Makro analyzer and O add-on module (Leco Corp.)
Y05	CEC <sup>1</sup>	cmol flask <sup>-1</sup>	Cation Exchange Capacity	
Y06	FastCpool <sup>2</sup>	g flask <sup>-1</sup>	Biochar fast mineralised labile C pool	
Y07	HrC <sup>1</sup>	Ratio: No scaling	Elemental ratios derived from Elemental analysis	
Y08	N:C <sup>1</sup>			
Y09	O:C <sup>1</sup>			
Y10	BPCA:C <sup>3</sup>		Ratio of total aromatic bound C to total elemental C. BPCA:C is an indicator of condensation.	Benzene polycarboxylic acid method. derived from Mid Infrared (MIR) analysis.
Y11	B6CA:C <sup>3</sup>		Ratio of full 6 carbon bound to elemental C. B6CA:C is an indicator of aromaticity.	
Y12	Ali-CH:Aro-CH <sup>3</sup>		The ratio of aliphatic CH to Aromatic CH	

<sup>a</sup> X block measurements were made using the incubation system and were recorded per flask. Y block measurements are biochar properties calculated on a dose per flask basis where possible. All the values and methods for the Y block variables were taken: <sup>1</sup> Budai et al. (2014)<sup>2</sup> Budai et al. (2016)<sup>3</sup> Budai et al. (2017). Ratios were not scaled to dose.

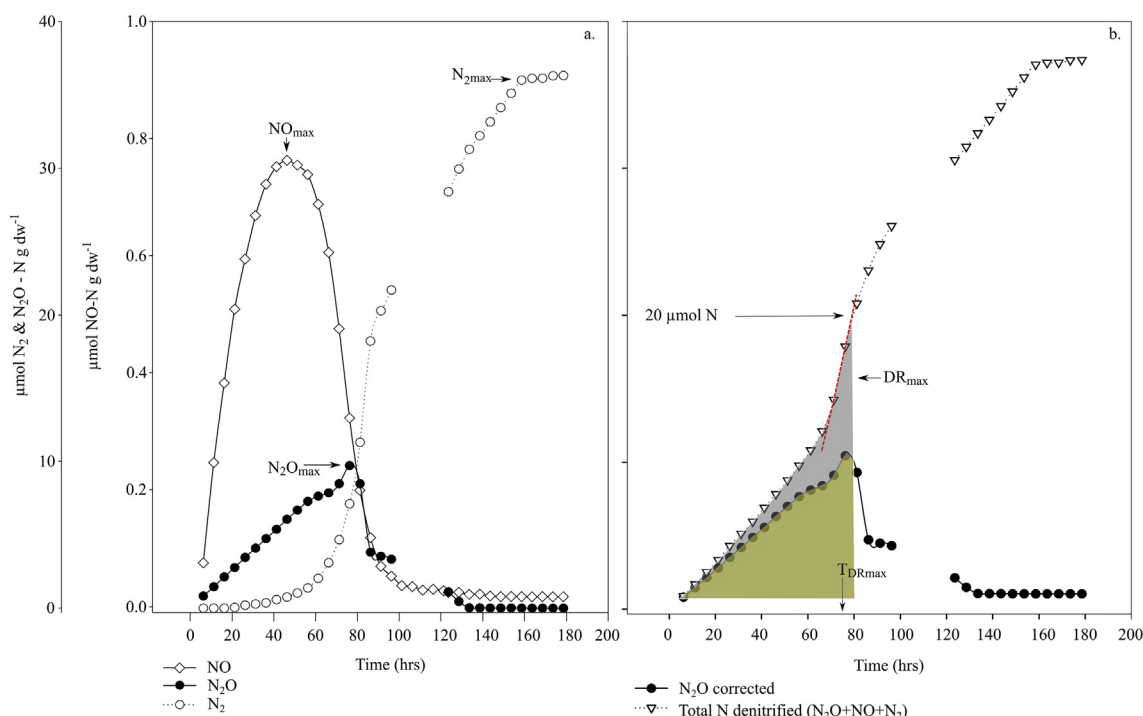


**Fig. 1.** Gas kinetics (a: NO, N<sub>2</sub>O, N<sub>2</sub>; b: N<sub>2</sub>O, NO + N<sub>2</sub>O + N<sub>2</sub>) and derived denitrification parameters in peat soil BC372 10% wt/wt (single bottle values). N<sub>2</sub> values in Fig. 1a are corrected for sampling loss, leakage and desorption whereas the transient accumulation of the intermediates NO and N<sub>2</sub>O are shown uncorrected. In Fig. 1b both N<sub>2</sub>O and NO + N<sub>2</sub>O + N<sub>2</sub> are corrected for sampling loss to derive the integrated product ratio (IPR) from the integrals with a cut off of 20  $\mu\text{mol N g dw soil}^{-1}$  total denitrification. Denitrification parameters shown in Fig. 1a are NO<sub>max</sub>, N<sub>2</sub>O<sub>max</sub> and N<sub>2</sub>max and in Fig. 1b, DR<sub>max</sub>, TDR<sub>max</sub> and IPR. The shading signifies the

properties as response variables and denitrification indices as independent variables, as this allowed us to examine the distribution of treatments based on denitrification indices in the X matrix without imposing the highly structured values describing the pyrolysis gradient. This was appropriate since we do not intend to use the PLSR for predicting denitrification responses, but rather for exploring correlations between denitrification indices and biochar properties. Models were first built without the control soils, before subsequently projecting the control soil samples into this model. In this way we show the relation of the control soils to the biochar treatments without the lack of biochar properties in the control soils defining the model. Model fit was judged by comparing the calibrated and validated explained variance in Y. All models were fit using the pls package in R (Mevik et al., 2015; R Core Team, 2017).

### 3. Results

#### 3.1. Effect of biochar HTT

In peat, the response of the IPR to biochar varied with HTT (Fig. 2a); FS105 and BC372 strongly increased IPR at doses above 1%, BC416 had no effect, while BC562 and 796 strongly decreased IPR. Hence, the N<sub>2</sub>O product ratio of peat displayed a marked threshold with respect to HTT in the range between 372 and 562 °C, where the effect shifted from increasing to repressing N<sub>2</sub>O production relative to total denitrification. In the mineral soil, biochars strongly reduced IPR independent of their HTT. Only the high (20%) dose of feedstock (FS105) increased the IPR (Fig. 2d). In non-amended controls, peat had a large innate N<sub>2</sub>O product ratio, while mineral soil produced little N<sub>2</sub>O and had a small innate N<sub>2</sub>O product ratio.

Biochars had little effect on the maximum denitrification rate (DR<sub>max</sub>) in the carbon-rich peat soil except for the two highest doses of FS105 and BC416, which stimulated denitrification (Fig. 2b). Maximum denitrification was reached earlier with high-temperature biochars

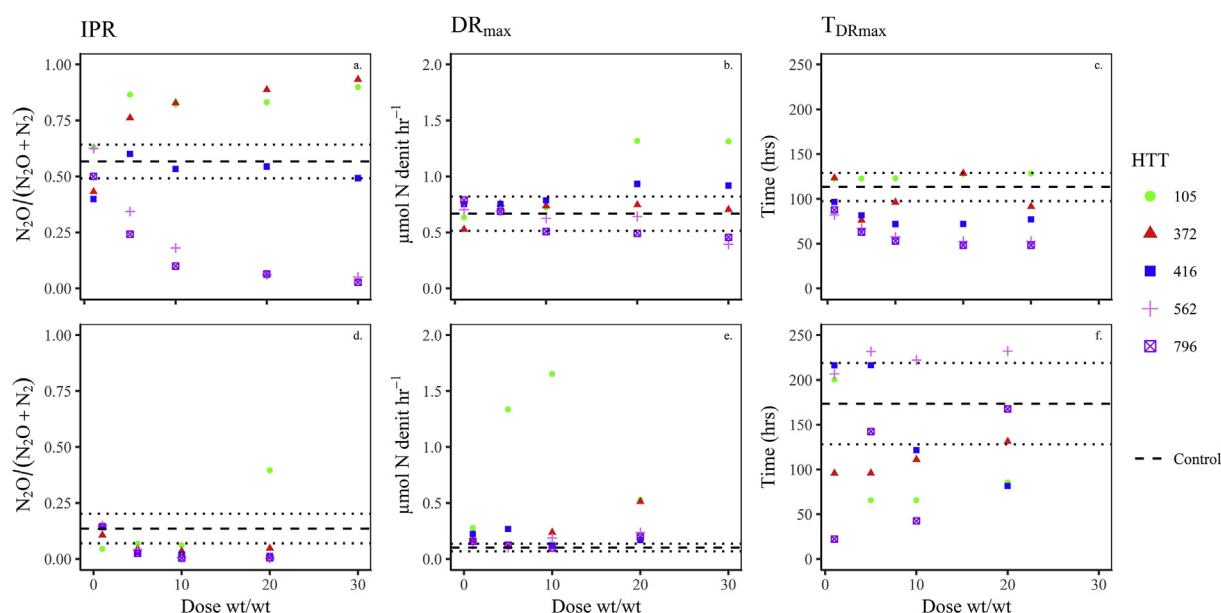
(Fig. 2c) in the acid peat soil. By contrast, denitrification in the mineral soil was stimulated by low HTT biochar, particularly by BC372, and the feedstock (Fig. 2e), without affecting the time needed to reach maximum denitrification activity (Fig. 2f).

Fig. 3 summarizes the effect of biochar addition on maximum N<sub>2</sub>O and NO accumulation over all HTT treatments and doses. N<sub>2</sub>O and NO accumulation was consistently reduced relative to the non-amended control when biochar produced at 562 °C and 796 °C was added to either soil, with a maximum reduction in N<sub>2</sub>O accumulation of 89% observed in peat soil with 30% w/w BC796 and of 98% with 20% w/w BC796 in the mineral soil (Fig. 3). The mineral soil accumulated approximately ten times less N<sub>2</sub>O than the peat soil (Fig. S4a, b). Interestingly, even the low-temperature biochar BC372 and low doses of FS105 reduced N<sub>2</sub>O accumulation in the mineral soil, which was not the case for the peat (Fig. 3). Likewise, NO and N<sub>2</sub>O accumulation in response to BC416 differed between soils. In peat, BC416 reduced NO accumulation but had little effect on N<sub>2</sub>O, whereas the opposite was the case in mineral soil. BC372 and FS105 stimulated N<sub>2</sub>O accumulation in the peat but reduced it in the mineral soil except for the 20% w/w dose of FS105. Thus, the N<sub>2</sub>O and NO response appeared to be soil dependent for biochar produced at or below 416 °C.

#### 3.2. Effect of biochar dose

In both soils, IPR responded strongly to biochar dose in the range of 1–5% w/w (Fig. 2a, d). Increasing the dose above 5% resulted in increasingly smaller response, irrespective of whether the effect was an increase or a decrease. Increasing the dose of biochar consistently decreased the accumulation of both NO and N<sub>2</sub>O in the BC562 and BC796 treatments of both soils (Fig. 3 a, b). BC416 varied in its effect between the two soils, showing no dose effect on N<sub>2</sub>O accumulation in the peat soil while showing a dose effect comparable to the high temperature chars in the mineral soil. Higher application rates of FS105 and BC372 increased NO and N<sub>2</sub>O accumulation, particularly in the peat soil (Fig. 3





**Fig. 2.** Scatter plot showing selected denitrification variables (Integrated product ratio (IPR), Maximum denitrification rate ( $DR_{max}$ ) and Time needed to reach maximum denitrification ( $T_{DRmax}$ )) in slurries of peat (a, b, c) and mineral soil (d, e, f) amended with different corn cob HTT biochars plotted against dose. Mean values for control soils without biochar are represented along with the standard deviation ( $n = 3$ ) as dotted lines.

a, b).

### 3.3. Relationship to BC properties

PLSR models for both soils (Fig. 4a, c) confirmed the strong effect of pyrolysis temperature (HTT) on denitrification. HTT is represented by the first component in the model (Fig. 4a, component 1: X scores 77%, Y scores 60% explained variance, Fig. 3b, component 1: X scores 40%, Y scores 63% explained variance) with higher doses of BC372 and FS105 located at the left side of the plot and high temperature chars (BC416, 562 and 796) located to the right. For the peat, the second component (Fig. 4a, component 2: X scores 7%, Y scores 10% explained variance, Fig. 3b, component 2, X scores 22%, Y scores 9% explained variance) appears to represent biochar dose, with low doses located at the top and high doses located towards the bottom of the score plot. In the mineral soil, this trend was much less apparent, reflecting the variability between the two soils in the overall effect strength of dose. The higher

overall explained variance in both Y and X in the first component shows that the effect of temperature treatment prevailed over the effect of dose in affecting denitrification kinetics. The central grouping of the control soils (which were subsequently projected onto the model) and the 1% dose treatments confirms that low-dose biochar treatment had little effect on denitrification kinetics since they contributed little to the variation explained by component 1 and 2. The loading plots (Fig. 4b) revealed that in the peat, all denitrification indices except for the  $NO:N_2O$  ratio were strongly positively correlated with H:C, O:C and the alicH:aroCH ratio, and strongly negatively correlated with BPCA, B6CA, pH and SA (Fig. 4b). In the mineral soil, the correlation structure was similar, except for  $T_{DRmax}$  (Fig. 4d). FastCpool appeared to play a more significant role in the minerals soil, while the opposite was true for SA. In the peat, measurements of denitrification activity,  $DR_{max}$  and  $T_{DRmax}$ , were strongly negatively correlated to SA and pH along component 1, respectively, whereas in the less active mineral soil,  $DR_{max}$  was strongly negatively correlated to pH and less so to SA.  $T_{DRmax}$

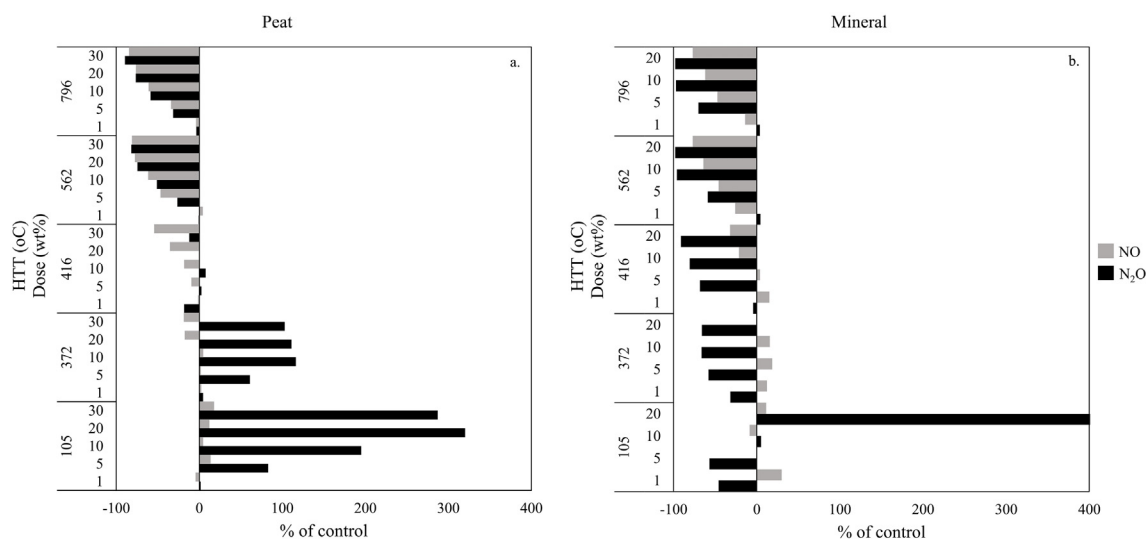


**Fig. 3.** Effect of biochar addition on maximum  $N_2O$  and  $NO$  accumulation in anoxic batch incubations of peat and mineral soil. The values are calculated as relative difference from the un-amended control (in %).

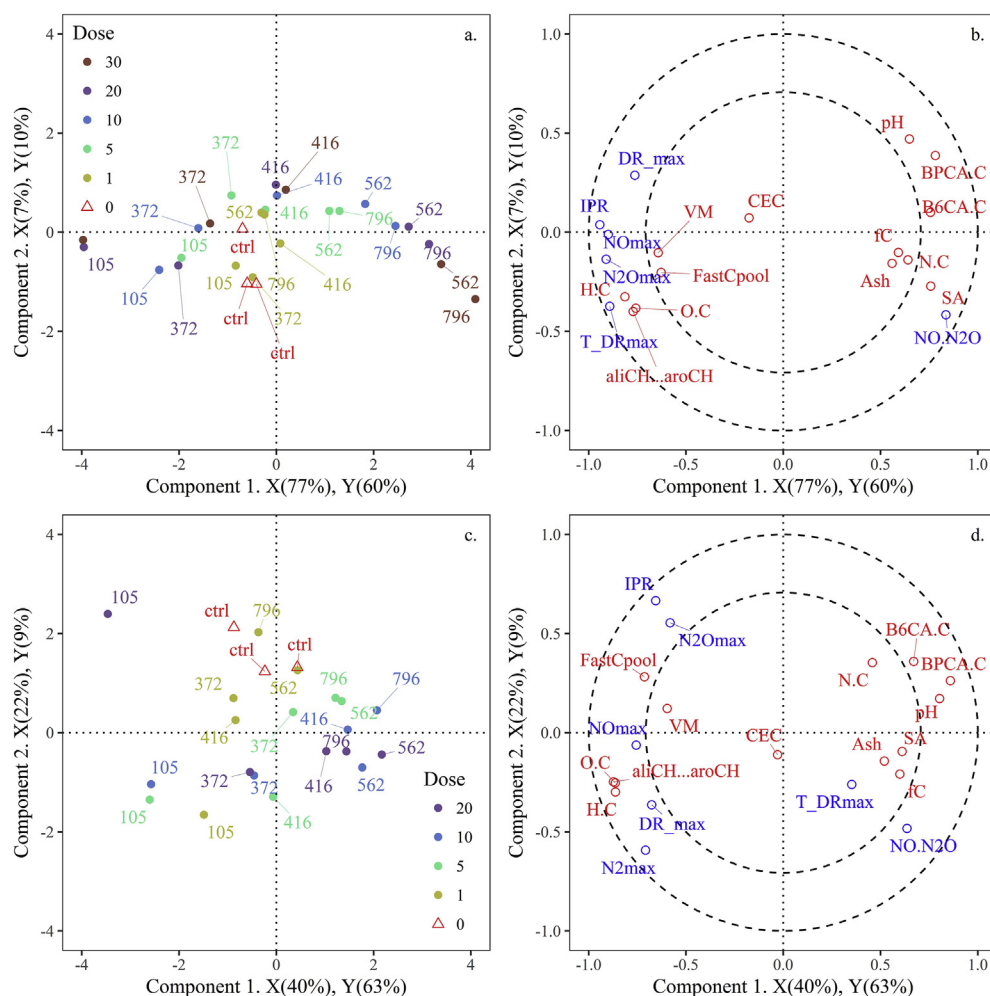


**Fig. 4.** PLSR models for peat (top: a & b.) and mineral soil (bottom: c & d). X scores plots (left a & c.) represent the objects/rows in matrix X and Y and show how the objects relate to one another in the multivariate space spanned by the model. X & Y correlation loading plots (right b & d) show the X (explanatory, blue) and Y (response, red) correlation loadings. The X & Y loading plot represents percent explained variance of each variable, variables within the inner circle have less than 50% of variance explained by the components, variables within the outer ring have greater than 50% variance explained by the 2 plotted components. Variables close to one another on this plot are highly positively correlated for the part of the data explained by the 2 components. (For interpretation of the references to colour in this figure legend, the reader is referred to the Web version of this article.)

played no role in the mineral soil owing to the lack of exponential product accumulation in this soil.

Biochar pH was highly negatively correlated with maximum NO and N<sub>2</sub>O accumulation in both soils and positively correlated with the ratio of NO to N<sub>2</sub>O along component 1, which increased with increasing pyrolysis temperature and dose in both soils (Fig. S7). SA, which was scaled to flask, showed a strong positive correlation with NO:N<sub>2</sub>O in the peat, but a somewhat weaker correlation in the mineral soil. VM and CEC had little impact on the correlation structure in both soils. The FastCpool which mainly represents the large labile carbon pool in the feedstock, appeared to play a more significant role for NO and N<sub>2</sub>O accumulation in the mineral than the peat soil.

N<sub>2max</sub> was removed from the peat model since added N was completely transformed to N<sub>2</sub> in all treatments (Fig. S4a), i.e. reaching close to mass balance between added and recovered gaseous N. By contrast, in the mineral soil, analyses of residual NO<sub>3</sub><sup>-</sup> and NO<sub>2</sub><sup>-</sup> post-incubation (Fig. S3) revealed that denitrification was incomplete for treatments with high-temperature chars and low doses of BC372. Interestingly, less gaseous N was recovered with high doses of FS105 and BC372 despite complete conversion, indicating immobilization or sorption of added NO<sub>3</sub><sup>-</sup>-N. Therefore, N<sub>2max</sub> was positively correlated with biochar properties representing C availability (FastCpool, aliCH:aroCH, O:C and H:C) and negatively with properties indicating the degree of carbonisation (B6CA:C, BPCA:C) in the mineral soil (Fig. 4d).

In the mineral soil only the 20% w/w dose of BC372 and all doses of FS105 induced exponential N<sub>2</sub> accumulation indicative of denitrifier growth (Fig. S4b). In the peat, all biochar treatments showed exponential N<sub>2</sub> accumulation, which, however, differed strongly with

biochar HTT (Fig. S4a). The onset of exponential production occurred earlier with high HTT chars, which was well captured by T<sub>DRmax</sub>, i.e. the time needed to achieve the steepest slope of N<sub>2</sub> production. N<sub>2</sub> accumulation eventually changed to linear accumulation (Fig. S4a) suggesting that denitrifier growth became substrate limited. This change occurred earlier with high temperature chars (Fig. S4a). No such linear phase in product accumulation was seen in peat soil amended with feedstock and the highest doses (20 and 30%) of BC372 (Fig. S4a).

## 4. Discussion

### 4.1. Which process dominated nitrate reduction?

We assert that the predominant NO<sub>3</sub><sup>-</sup> reduction pathway in our flasks was denitrification, even though there exist a number of alternative pathways (DNRA, anammox, chemodenitrification, co-denitrification) dissipating NO<sub>3</sub><sup>-</sup> under anoxic conditions. Both DNRA and anammox are favoured by high pH (Zhang et al., 2015) and are considered to be of limited significance in well drained upland soils (Schmidt et al., 2011; Ligi et al., 2015; Xi et al., 2016). Anammox, in particular, requires the accumulation of nitrite (Long et al., 2013), which only occurs in moderately acidic to alkaline soil. The mineral soil incubations accumulated considerable amounts of NO<sub>2</sub><sup>-</sup> (Fig. S3) concomitant with rising pH in the slurries (Fig. S5b), however, the fact that NO<sub>2</sub><sup>-</sup> accumulated at the end of the experiment suggests that NO<sub>2</sub><sup>-</sup> consumption by anammox was not the dominating process. Co-denitrification (Spott et al., 2011) may have been an important process in our peat due to the abundance of organic N moieties. However, we

assume that the utilisation of this additional N source would have altered the mass balance of recovered  $\text{N}_2\text{-N}$  relative to the added  $\text{NO}_3^- \text{-N}$ . Since we did not see this in our incubations with the peat soil, we assume that co-denitrification was negligible. Chemodenitrification, i.e. the dismutation of protonized nitrite ( $\text{HNO}_2$ ) to  $\text{NO}$  and  $\text{N}_2\text{O}$  and/or the reaction of  $\text{HNO}_2$  with redox active compounds on mineral surfaces cannot be ruled out and is addressed later in the discussion. A study by Wankel et al. (2017), however, suggested that in the presence of high  $\text{NO}_3^-$  concentrations, bacterial and fungal denitrifiers are likely to dominate  $\text{N}_2\text{O}$  and  $\text{N}_2$  production. For these reasons we are confident that the dominating process of  $\text{NO}_3^-$  consumption in our experiments was canonical denitrification, with minor interference from other  $\text{NO}_3^-/\text{NO}_2^-$  dissipating processes.

#### 4.2. Biochar produced at high temperature reduces $\text{N}_2\text{O}$ and $\text{NO}$ emission

Accumulation of  $\text{N}_2\text{O}$  and  $\text{NO}$  was consistently reduced when corncob biochars produced at 562 °C and 796 °C were added to either soil. Our results do not allow us to define a precise HTT threshold responsible for this effect, however 416 °C appeared to be a pyrolysis temperature above which there was a neutral to suppressing effect on  $\text{NO}$  and  $\text{N}_2\text{O}$  release in both soils (Fig. 2). The two biochars which reduced  $\text{N}_2\text{O}$  and  $\text{NO}$  the most were the ones with the highest degree of carbonisation as indicated by low H:C, O:C, aliCH:aroCH and high BPCA:C and B6CA:C ratios (Table 2). In a meta-analysis, Cayuela et al. (2015) found that a biochar H:C ratio < 0.3 is a good predictor for  $\text{N}_2\text{O}$  suppression. We found consistent  $\text{N}_2\text{O}$  suppression with BC562 and BC796, which had H:C values of 0.37 and 0.13, respectively, while BC416, which showed an inconsistent effect had a H:C ratio of 0.59. Therefore our results support the concept of H:C being a predictor for suppression of  $\text{N}_2\text{O}$  emissions from denitrification and extend this concept to  $\text{NO}$  emissions. Our results also suggest that there is a plateau in the mitigation potential beyond a specific HTT as evidenced by the quite similar responses to BC562 and BC796.

Pronounced  $\text{NO}$  and  $\text{N}_2\text{O}$  suppression in the presence of high temperature chars points towards several key properties involved in  $\text{N}_2\text{O}$  suppression. Carbonisation and aromaticity (BPCA:C, aliCH:aroCH) as well as condensation (B6CA:C) increase with increasing HTT and condensed polyaromatic structures of chars have been shown to carry electro-chemical properties (Klöpfer et al., 2014a), which may facilitate redox reactions taking place during denitrification (Chen et al., 2018). However, in our study, increasing degree of carbonisation also correlated positively with other properties such as ash content, pH and SA. The high correlation of SA with indicators of denitrification in the peat soil and pH in both soils suggests that pH and SA could be causally involved in  $\text{N}_2\text{O}$  suppression by biochar.

SA was negatively correlated with  $\text{NO}$  and  $\text{N}_2\text{O}$  accumulation and positively with the ratio of  $\text{NO}:\text{N}_2\text{O}$ . SA, which has been proposed as a proxy for the sorption capacity of biochar for organic compounds (Hale et al., 2016), may increase  $\text{NO}$  and  $\text{N}_2\text{O}$  reduction rates by concentrating these denitrification intermediates locally around chars thus increasing the effective concentration for the catalytic reaction (Harter et al., 2016). Interestingly, the effect of higher temperature chars in the peat soil was larger for  $\text{N}_2\text{O}$  than  $\text{NO}$ , suggesting a stronger relative effect of biochar on  $\text{N}_2\text{O}$  than  $\text{NO}$  accumulation (Fig S7). The shape of the SA response to pyrolysis temperature for our biochars differs substantially from that of H:C or pH (Budai et al., 2014), and is defined by a peak in SA at BC562 followed by a reduction at BC796. Although it has been shown that biochar can permanently sorb  $\text{N}_2\text{O}$  under anhydrous conditions (Cornelissen et al., 2013), this was probably not the case in our soil slurries as plateauing  $\text{N}_2\text{-N}$  accumulation in peat incubations indicated that  $\text{N}_2\text{O-N}$  was fully denitrified. Our results instead support the hypothesis of Harter et al. (2016), who argued that the ability of biochar to sorb  $\text{N}_2\text{O}$  transiently increases its residency time and local concentration, thereby facilitating microbial reduction.

Biochar pH appeared to be another key variable linked to  $\text{NO}$  and

$\text{N}_2\text{O}$  suppression, as indicated by the opposite position of these two variables in the PLSR loading plots (Fig. 4). Over the range of pyrolysis temperatures, the  $\text{pH}_{\text{H}_2\text{O}}$  of our biochar, measured in water, plateaued at 416 °C with a value of 10.07 (Table 2). Despite highest pH in the BC416 treatment, measurements of slurry pH after 182–235 h of stirred anoxic incubation showed a strong linear correlation between pH and ash content of the biochar that increased with pyrolysis temperature through the entire range of BC pyrolysis temperatures (Fig. S6). This suggests that biochar ash contributed significantly to the observed alkalisation, likely owing its high proportion of secondary carbonates and base cations (Yuan et al., 2011). The liming effect of biochar in acidic soils can strongly reduce  $\text{NO}$  accumulation by repressing the chemical dismutation of nitrous acid ( $\text{HNO}_2$ ), the protonated form of  $\text{NO}_2^-$ , to  $\text{NO}$  (Chalk and Smith, 1983). Low pH is also known to impair  $\text{N}_2\text{O}$  reductase ( $\text{N}_2\text{OR}$ ), the enzyme responsible for  $\text{N}_2\text{O}$  reduction, with increasing inhibitory effects below pH 6.1 (Liu et al., 2014; Brenzinger et al., 2015). However, in our study, while the pH of the biochar strongly correlated with denitrification indices, the ash content did not (Fig. 4). This may be because the ash content can have confounding effects on other variables influencing denitrification. For instance, it has been suggested that ash can result in salting out of  $\text{N}_2\text{O}$  from solution, which would increase  $\text{N}_2\text{O}$  release (Yanai et al., 2007).

#### 4.3. Biochar prepared at low temperature has contrasting effects on $\text{N}_2\text{O}$ emission in mineral soil and peat

The low-temperature char (BC372) was characterized by a low degree of carbonisation and high O:C and H:C ratios, high VM and low ash content. Stimulation of  $\text{N}_2\text{O}$  emissions by low-temperature chars has been reported previously (Kammann et al., 2012; Li et al., 2013). A re-analysis of the data synthesized in Cayuela et al. (2015) shows that high H:C chars have a potential to stimulate  $\text{N}_2\text{O}$  emissions ( $p < 0.01$ , SI section 4). However, this effect appears to be less clear-cut than the < 0.3 threshold for  $\text{N}_2\text{O}$  suppression, suggesting that there are other, interacting factors modulating the relationship between H:C > 0.3 and  $\text{N}_2\text{O}$  emission.

The contrasting effects of low temperature char (BC372) and feedstock (FS105) on  $\text{N}_2\text{O}$  accumulation in the two soils suggests that soil properties interacted with biochar in its effect on denitrification. The most obvious differences between peat and mineral soil were carbon content (53.0 vs 2.8%), C/N ratio (29.5 vs. 9.8), CEC (1480 vs. 51  $\text{cmol kg}^{-1}$ ) and  $\text{pH}_{\text{H}_2\text{O}}$  (5.1 vs 5.9). Surprisingly, low-temperature char and feedstock increased  $\text{N}_2\text{O}$  accumulation in the carbon-rich peat, which supported high denitrification rates, indicating ample decomposable carbon. One would expect that adding low-temperature char and feedstock, with their relatively large pool of readily decomposable carbon, to this carbon rich peat would have little or no effect on denitrification and its product stoichiometry. Studies have suggested that adding labile C to a system with limited biologically available carbon would increase the reductant-to-oxidant ratio ( $\text{DOC}:\text{NO}_3^-$ ), which should result in more complete denitrification (Senbayram et al., 2012). This mechanism could explain the observed kinetics in the mineral soil where low temperature char and feedstock caused an increase in total denitrification (Fig S4b, S3) accompanied by an overall reduction in  $\text{N}_2\text{O}$  accumulation (Fig. 3b). A closer inspection of the  $\text{N}_2$  kinetics of peat revealed that the FS105 and BC372 treatments accumulated  $\text{N}_2$  much slower than the treatments with high-temperature chars (Fig. S4b). Accordingly,  $T_{\text{DRmax}}$ , the time needed to express maximum denitrification activity, was larger and positively correlated with indices of low carbonisation degree (Fig. 4b). While the faster increase in denitrification activity with high-temperature chars may be explained by their stronger alkalinizing effect (Fig. S5), it is unclear which properties of low-temperature biochar and feedstock caused this delay. Acid peat soils are known to harbour denitrifier communities with low taxonomic diversity and hence limited metabolic versatility (Palmer et al., 2010; Braker et al., 2012; Dörsch et al., 2012). Addition of allochthonous C-



sources, in the form of dried corn cob or its low-temperature pyrolysis product, to anoxic incubations may have triggered growth of competing functional groups (e.g. fermenters). This may have initially repressed denitrifier activity, until denitrifier community composition changed (e.g. Brenzinger et al., 2015) and supported exponential  $N_2$  accumulation with high  $DR_{max}$  values and rapid  $N_2O$  uptake. We therefore tentatively attribute the  $N_2O$  stimulating effect of low-temperature corncob biochar and its feedstock to some unidentified disruption of initial denitrification activity resulting in transiently incomplete denitrification.

#### 4.4. Biochar and denitrification: which biochar properties matter?

The significant variables for explaining the  $N_2O$  mitigation effect of biochar in our study were carbonisation indices, pH and SA (Fig. 4 b, d). Carbonisation indices encapsulate concurrent changes in biochar properties: 1) disappearance of labile organic carbon with increasing temperature, and 2) formation and condensation of aromatic structures with increasing temperatures. This implies that one must consider the effects of both labile organic carbon structures at low pyrolysis temperature and condensed aromatic sheet formation at higher temperature when assessing potential biochar effects on denitrification.

Aromatic structures of chars formed at higher pyrolysis temperature have been shown to alter the electro-chemical properties of biochar (Klöpfer et al., 2014a) which can mediate redox reactions (Kappler et al., 2014; Chen et al., 2018). Our experiment does not provide direct evidence for this effect, but the more efficient denitrification, represented by smaller  $T_{DRmax}$  and lower accumulation of intermediates, could be due to redox reactions mediated directly by the biochar. In a peat soil, however, which contains abundant redox active components (Klöpfer et al., 2014b), it is unlikely that the addition of biochar would have a measurable impact on these processes.

The effect of pH on heterotrophic denitrification is well established (as reviewed in Blum et al., 2018). pH affects not only the accumulation of intermediates (Kappelmeyer et al., 2003) but low pH is also well documented to inhibit the reduction of  $N_2O$  to  $N_2$  (Šimek and Cooper, 2002; Bakken et al., 2012). Low pH does not affect the transcription of *nosZ*, the gene encoding for  $N_2O$  reductase, but its functioning appears to be impaired post-transcriptionally (Bergaust et al., 2010). The pH of both of our soils was lower than the pH threshold of 6.1 for fully functional  $N_2O$  reductase proposed by Liu et al. (2010) and Brenzinger et al. (2015), i.e. pH 5.86 for the mineral soil and 5.08 for the peat (Table 1). However, the pH of the anoxic slurries increased as denitrification progressed, surpassing this threshold (Fig. S5). The peat was more buffered, with a higher CEC (Table 1), than the mineral soil (Fig. S6), which probably explains why the pH in biochar treatments of the peat soil was more highly correlated with IPR and  $T_{DRmax}$  and with the total accumulation of intermediates, i.e.  $NO_{max}$  and  $N_2O_{max}$  (Fig. 4 b). The higher buffering capacity of the peat also resulted in a more progressive denitrification response to pH over the full range of dose (Fig. 3). The strong negative correlation between  $T_{DRmax}$  and pH (Fig. 4b) shows that biochar accelerated the induction of a measurable  $N_2O$  reduction.

Biochar SA is an indicator for the sorption capacity of biochar (Hale et al., 2015) and is a result of the concurrent loss of amorphous carbon and the development of graphitic structures and highly reduced surface functional groups. There are several potential mechanisms by which biochar SA could affect denitrification. Cornelissen et al. (2013) proposed permanent sorption of  $N_2O$  to biochar surfaces. Others have suggested that biochar can sorb DOC, reducing access to electron donors (Lu et al., 2014). Because we see no effect of high SA biochar on the recovery of added N, our results support neither permanent sorption of  $N_2O$  nor reduced access to DOC as mechanisms. By contrast, our results support the hypothesis of more complete denitrification due to increased residency time of  $N_2O$  on or near biochar surfaces through temporary sorption (Harter et al., 2016). Along with the other

mechanisms we have discussed, such as pH and carbonisation degree, this could explain the positive correlation we observed between  $NO$  and  $N_2O$  suppression and SA of the biochars (Fig. 4b).

In summary, we used a well-characterized biochar temperature series with continuously scaled properties in standardized denitrification assays to examine which biochar properties are responsible for the observed effect of biochar on  $N_2O$  emissions from denitrification. Our results suggest that biochar effects on  $N_2O$  emissions from denitrification are variable, or even contrasting, depending on which soils are used. Biochar from a single feedstock type can shift from stimulating  $N_2O$  emissions to reducing them over a relatively small range of HTT, highlighting that the  $N_2O$  effect of biochar is likely not caused by a single property of the biochar. We further show that biochar is interacting not only with the final reduction step of denitrification but may also impact total denitrification.

Contrary to our highly standardized experimental design, environmental conditions in bulk soil vary substantially in time and space. *In situ*  $N_2O$  emissions are highly variable in time, driven by events such as fertilization, rewetting, tillage or freeze-thaw. In these conditions periods of high emissions can last over several days and are likely driven by denitrification (Flessa et al., 1995). While the effect of biochar on event-driven  $N_2O$  emissions is largely unknown (Edwards et al., 2018), our study focuses primarily on denitrifier response to longer lasting anoxia in the presence of biochar. Our study shows how biochar interacts with denitrification and potentially lowers the  $N_2O$  product ratio under those conditions. We demonstrate a link between biochar properties and denitrification functioning for one specific corncob feedstock. We are confident that our results with corncob biochar are relevant for a range of other biochars, as we have shown previously that corncob biochar is comparable in chemical and physical properties to those produced from other grass feedstocks over wide ranges of pyrolysis temperature (Budai et al., 2014, 2017). However, key response variables highlighted in our study, such as SA and pH, can be manipulated not only through feedstock selection but also through post-processing of biochar products (Chintala et al., 2013; Rajapaksha et al., 2016). Because substantial reduction of  $N_2O$  emission from agricultural soils is needed, future investigations should specifically target the effects of biochar-property enhancement, thereby supporting the transition from mechanistic understanding to pilot implementation.

#### Declaration of interests

None.

#### Acknowledgments

We are very grateful to Trygve Fredriksen, Jan Erik Jacobsen and Lars Molstad for technical support and guidance in the laboratory and to Matthew Weldon for statistical advice both early in the process and during revisions. We are also grateful to Lars Bakken for providing methods for measuring nitrite and nitrate as well as early comments on the experimental design. We would also like to thank the editor and the two reviewers for constructive comments that helped to improve the quality of this article. This work was supported through a stipend provided by the “Stiftelsen fondet for jord-og myrundersøkelser”. Partial funding for this research was provided by the Norwegian Ministry of Climate and Environment through the NIBIO SIS-Jordkarbon project and by the Research Council of Norway through the Carbo-Fertil project NFR281113. PD received funding from the FACCE-ERA-GAS project MAGGE-pH under the Grant Agreement No. 696356.

#### Appendix A. Supplementary data

Supplementary data to this article can be found online at <https://doi.org/10.1016/j.soilbio.2019.04.018>.

## References

- Ameloot, N., Graber, E.R., Verheijen, F.G.A., De Neve, S., 2013. Interactions between biochar stability and soil organisms: review and research needs. *European Journal of Soil Science* 64, 379–390.
- Antal, M.J., Gronli, M., 2003. The art, science, and technology of charcoal production. *Industrial & Engineering Chemistry Research* 42, 1619–1640.
- Bakken, L.R., Bergaust, L., Liu, B., Frostegård, Å., 2012. Regulation of denitrification at the cellular level: a clue to the understanding of N<sub>2</sub>O emissions from soils. *Philosophical Transactions of the Royal Society B: Biological Sciences* 367, 1226–1234.
- Bergaust, L., Mao, Y., Bakken, L.R., Frostegård, Å., 2010. Denitrification response patterns during the transition to anoxic respiration and posttranscriptional effects of sub-optimal pH on nitrogen oxide reductase in *Paracoccus denitrificans*. *Applied and Environmental Microbiology* 76, 6387–6396.
- Blum, J.-M., Su, Q., Ma, Y., Valverde-Pérez, B., Domingo-Félez, C., Jensen, M.M., Smets, B.F., 2018. The pH dependency of N-converting enzymatic processes, pathways and microbes: effect on net N<sub>2</sub>O production. *Environmental Microbiology* 20, 1623–1640.
- Borchard, N., Schirrmann, M., Cayuela, M.L., Kammann, C., Wrage-Mönnig, N., Estavillo, J.M., Fuentes-Mendizábal, T., Sigua, G., Spokas, K., Ippolito, J.A., Novak, J., 2019. Biochar, soil and land-use interactions that reduce nitrate leaching and N<sub>2</sub>O emissions: a meta-analysis. *The Science of the Total Environment* 651, 2354–2364.
- Braker, G., Dörsch, P., Bakken, L., 2012. Genetic characterization of denitrifier communities with contrasting intrinsic functional traits. *FEMS Microbiology Ecology* 79, 542–554.
- Brenzinger, K., Dörsch, P., Braker, G., 2015. pH-driven shifts in overall and transcriptionally active denitrifiers control gaseous product stoichiometry in growth experiments with extracted bacteria from soil. *Frontiers in Microbiology* 6.
- Budai, A., Wang, L., Gronli, M., Strand, L.T., Antal, M.J., Abiven, S., Dieguez-Alonso, A., Anca-Couce, A., Rasse, D.P., 2014. Surface properties and chemical composition of corn cob and miscanthus biochars: effects of production temperature and method. *Journal of Agricultural and Food Chemistry* 62, 3791–3799.
- Budai, A., Rasse, D.P., Lagomarsino, A., Lerch, T.Z., Paruch, L., 2016. Biochar persistence, priming and microbial responses to pyrolysis temperature series. *Biology and Fertility of Soils* 1–13.
- Budai, A., Calucci, L., Rasse, D.P., Strand, L.T., Pengerud, A., Wiedemeier, D., Abiven, S., Forte, C., 2017. Effects of pyrolysis conditions on Miscanthus and corn cob chars: characterization by IR, solid state NMR and BPCA analysis. *Journal of Analytical and Applied Pyrolysis* 128, 335–345.
- Case, S.D.C., McNamara, N.P., Reay, D.S., Whitaker, J., 2014. Can biochar reduce soil greenhouse gas emissions from a Miscanthus bioenergy crop? *Global Change Biology Bioenergy* 6, 76–89.
- Cayuela, M.L., Sánchez-Monedero, M.A., Roig, A., Hanley, K., Enders, A., Lehmann, J., 2013. Biochar and denitrification in soils: when, how much and why does biochar reduce N<sub>2</sub>O emissions? *Scientific Reports* 3, 1732.
- Cayuela, M.L., van Zwieten, L., Singh, B.P., Jeffery, S., Roig, A., Sánchez-Monedero, M.A., 2014. Biochar's role in mitigating soil nitrous oxide emissions: a review and meta-analysis. *Agriculture, Ecosystems & Environment* 191, 5–16.
- Cayuela, M.L., Jeffery, S., van Zwieten, L., 2015. The molar H:C<sub>org</sub> ratio of biochar is a key factor in mitigating N<sub>2</sub>O emissions from soil. *Agriculture, Ecosystems & Environment* 202, 135–138.
- Chalk, P.M., Smith, C.J., 1983. Chemodenitrification. In: Freney, J.R., Simpson, J.R. (Eds.), *Gaseous Loss of Nitrogen from Plant-Soil Systems*. Springer Netherlands, Dordrecht, pp. 65–89.
- Chen, G., Zhang, Z., Zhang, Z., Zhang, R., 2018. Redox-active reactions in denitrification provided by biochars pyrolyzed at different temperatures. *The Science of the Total Environment* 615, 1547–1556.
- Chintala, R., Mollinedo, J., Schumacher, T.E., Papiernik, S.K., Malo, D.D., Clay, D.E., Kumar, S., Gulbrandson, D.W., 2013. Nitrate sorption and desorption in biochars from fast pyrolysis. *Microporous and Mesoporous Materials* 179, 250–257.
- Clough, T.J., Bertram, J.E., Ray, J.L., Condon, L.M., O'Callaghan, M., Sherlock, R.R., Wells, N.S., 2010. Unweathered wood biochar impact on nitrous oxide emissions from a bovine-urine-amended pasture soil. *Soil Science Society of America Journal* 74, 852–860.
- Cornelissen, G., Rutherford, D.W., Arp, H.P.H., Dörsch, P., Kelly, C.N., Rostad, C.E., 2013. Sorption of pure N<sub>2</sub>O to biochars and other organic and inorganic materials under anhydrous conditions. *Environ. Sci. Technol.* 47, 7704–7712.
- Dörsch, P., Braker, G., Bakken, L.R., 2012. Community specific pH response of denitrification: experiments with cells extracted from organic soils. *FEMS Microbiology Ecology* 79, 530–541.
- Edwards, J.D., Pittelkow, C.M., Kent, A.D., Yang, W.H., 2018. Dynamic biochar effects on soil nitrous oxide emissions and underlying microbial processes during the maize growing season. *Soil Biology and Biochemistry* 122, 81–90.
- Firestone, M.K., Davidson, E.A., 1989. *Microbiological Basis of NO and N<sub>2</sub>O Production and Consumption in Soil*. University of California, Berkeley, CA 94720 (USA).
- Flessa, H., Dörsch, P., Beese, F., 1995. Seasonal variation of N<sub>2</sub>O and CH<sub>4</sub> fluxes in differently managed arable soils in southern Germany. *Journal of Geophysical Research: Atmosphere* 100, 23115–23124.
- Fungo, B., Guarena, D., Thiongo, M., Lehmann, J., Neufeldt, H., Kalbitz, K., 2014. N<sub>2</sub>O and CH<sub>4</sub> emission from soil amended with steam-activated biochar. *Journal of Plant Nutrition and Soil Science* 177, 34–38.
- Grutzmacher, P., Puga, A.P., Bibar, M.P.S., Coscione, A.R., Packer, A.P., de Andrade, C.A., 2018. Carbon stability and mitigation of fertilizer induced N<sub>2</sub>O emissions in soil amended with biochar. *The Science of the Total Environment* 625, 1459–1466.
- Hagemann, N., Kammann, C.I., Schmidt, H.-P., Kappler, A., Behrens, S., 2017. Nitrate capture and slow release in biochar amended compost and soil. *PLoS One* 12, e0171214.
- Hale, S.E., Endo, S., Arp, H.P.H., Zimmerman, A.R., Cornelissen, G., 2015. Sorption of the monoterpenes  $\alpha$ -pinene and limonene to carbonaceous geosorbents including biochar. *Chemosphere* 119, 881–888.
- Hale, S.E., Arp, H.P.H., Kupryianchyk, D., Cornelissen, G., 2016. A synthesis of parameters related to the binding of neutral organic compounds to charcoal. *Chemosphere* 144, 65–74.
- Harter, J., Guzman-Bustamante, I., Kuehfuss, S., Ruser, R., Well, R., Spott, O., Kappler, A., Behrens, S., 2016. Gas entrapment and microbial N<sub>2</sub>O reduction reduce N<sub>2</sub>O emissions from a biochar-amended sandy clay loam soil. *Scientific Reports* 6, 39574.
- Harter, J., El-Hadidi, M., Huson, D.H., Kappler, A., Behrens, S., 2017. Soil biochar amendment affects the diversity of nosZ transcripts: implications for N<sub>2</sub>O formation. *Scientific Reports* 7, 3338.
- He, Y., Zhou, X., Jiang, L., Li, M., Du, Z., Zhou, G., Shao, J., Wang, X., Xu, Z., Hosseini Bai, S., Wallace, H., Xu, C., 2017. Effects of biochar application on soil greenhouse gas fluxes: a meta-analysis. *GCB Bioenergy* 9, 743–755.
- Jia, J., Li, B., Chen, Z., Xie, Z., Xiong, Z., 2012. Effects of biochar application on vegetable production and emissions of N<sub>2</sub>O and CH<sub>4</sub>. *Soil Science & Plant Nutrition* 58, 503–509.
- Kammann, C., Ratering, S., Eckhard, C., Muller, C., 2012. Biochar and hydrochar effects on greenhouse gas (carbon dioxide, nitrous oxide, and methane) fluxes from soils. *Journal of Environmental Quality* 41, 1052–1066.
- Kappelmeyer, U., Kusch, P., Stottmeister, U., 2003. Model experiments on the influence of artificial humic compounds on chemodenitrification. *Water, Air, and Soil Pollution* 147, 317–330.
- Kappler, A., Wuestner, M.L., Ruecker, A., Harter, J., Halama, M., Behrens, S., 2014. Biochar as an electron shuttle between bacteria and Fe(III) minerals. *Environmental Science and Technology Letters* 1, 339–344.
- Kloss, S., Zehetner, F., Dellantonio, A., Hamid, R., Ottner, F., Liedtke, V., Schwanninger, M., Gerzabek, M.H., Soja, G., 2012. Characterization of slow pyrolysis biochars: effects of feedstocks and pyrolysis temperature on biochar properties. *Journal of Environmental Quality* 41, 990–1000.
- Klüpfel, L., Keilweil, M., Kleber, M., Sander, M., 2014a. Redox properties of plant biomass-derived black carbon (biochar). *Environ. Sci. Technol.* 48, 5601–5611.
- Klüpfel, L., Piepenbrock, A., Kappler, A., Sander, M., 2014b. Humic substances as fully regenerable electron acceptors in recurrently anoxic environments. *Nature Geoscience* 7, 195.
- Lehmann, J., Gaunt, J., R., M., 2006. Bio-char sequestration in terrestrial ecosystems - a review. *Mitigation and Adaptation Strategies for Global Change* 11, 403–427.
- Li, F., Cao, X., Zhao, L., Yang, F., Wang, J., Wang, S., 2013. Short-term effects of rice straw and its derived biochar on greenhouse gas emission in five typical soils in China. *Soil Science & Plant Nutrition* 59, 800–811.
- Ligi, T., Truu, M., Oopkaup, K., Nölvak, H., Mander, Ü., Mitsch, W.J., Truu, J., 2015. The genetic potential of N<sub>2</sub> emission via denitrification and ANAMMOX from the soils and sediments of a created riverine treatment wetland complex. *Ecological Engineering* 80, 181–190.
- Liu, B., Mørkvad, P.T., Frostegård, Å., Bakken, L.R., 2010. Denitrification gene pools, transcription and kinetics of NO, N<sub>2</sub>O and N<sub>2</sub> production as affected by soil pH. *FEMS Microbiology Ecology* 72, 407–417.
- Liu, B., Frostegård, Å., Bakken, L.R., 2014. Impaired reduction of N<sub>2</sub>O to N<sub>2</sub> in acid soils is due to a posttranscriptional interference with the expression of nosZ. *mBio* 5.
- Lorenz, K., Lal, R., 2014. Soil Organic Carbon Sequestration in Agroforestry Systems. A Review. *Agronomy for Sustainable Development*, vol. 34. pp. 443–454.
- Long, A., Heitman, J., Tobias, C., Philips, R., Song, B., 2013. Co-occurring anammox, denitrification, and codenitrification in agricultural soils. *Applied and Environmental Microbiology* 79, 168–176.
- Lu, W., Ding, W., Zhang, J., Li, Y., Luo, J., Bolan, N., Xie, Z., 2014. Biochar suppressed the decomposition of organic carbon in a cultivated sandy loam soil: a negative priming effect. *Soil Biology and Biochemistry* 76, 12–21.
- Martens, R., 1987. Estimation of microbial biomass in soil by the respiration method - importance of soil-pH and flushing methods for the measurement of respired CO<sub>2</sub>. *Soil Biology and Biochemistry* 19, 77–81.
- Mevik, B.-H., Wehrens, R., Liland, K.H., 2015. Pls: Partial Least Squares and Principal Component Regression. R package version 2.6-0. <https://CRAN.R-project.org/package=pls>.
- Molina-Herrera, S., Haas, E., Grote, R., Kiese, R., Klatt, S., Kraus, D., Kampffmeyer, T., Friedrich, R., Andreae, H., Loubet, B., Ammann, C., Horváth, L., Larsen, K., Gruening, C., Frumau, A., Butterbach-Bahl, K., 2017. Importance of soil NO emissions for the total atmospheric NOx budget of Saxony, Germany. *Atmospheric Environment* 152, 61–76.
- Molstad, L., Dörsch, P., Bakken, L.R., 2007. Robotized incubation system for monitoring gases (O<sub>2</sub>, N<sub>2</sub>O, N<sub>2</sub>) in denitrifying cultures. *Journal of Microbiological Methods* 71, 202–211.
- Molstad, L., Dörsch, P., Bakken, L., 2016. Improved Robotized Incubation System for Gas Kinetics in Batch Cultures. <https://doi.org/10.13140/RG.2.2.30688.07680>.
- Nadeem, S., Dörsch, P., Bakken, L.R., 2013. The significance of early accumulation of nanomolar concentrations of NO as an inducer of denitrification. *FEMS Microbiology Ecology* 83, 672–684.
- Nelissen, V., Saha, B.K., Ruysschaert, G., Boeckx, P., 2014. Effect of different biochar and fertilizer types on N<sub>2</sub>O and NO emissions. *Soil Biology and Biochemistry* 70, 244–255.
- Obia, A., Cornelissen, G., Mulder, J., Dörsch, P., 2015. Effect of soil pH increase by biochar on NO, N<sub>2</sub>O and N<sub>2</sub> production during denitrification in acid soils. *PLoS One* 10, e0138781.
- Palmer, K., Drake, H.L., Horn, M.A., 2010. Association of novel and highly diverse acid-

- tolerant denitrifiers with  $\text{N}_2\text{O}$  fluxes of an acidic fen. *Applied and Environmental Microbiology* 76, 1125–1134.
- Pourhashem, G., Rasool, Q.Z., Zhang, R., Medlock, K.B., Cohan, D.S., Masiello, C.A., 2017. Valuing the air quality effects of biochar reductions on soil NO emissions. *Environ. Sci. Technol.* 51, 9856–9863.
- R Core Team, 2017. *R: A Language and Environment for Statistical Computing*. R Foundation for Statistical Computing, Vienna, Austria URL: <https://www.R-project.org/>.
- Rajapaksha, A.U., Chen, S.S., Tsang, D.C.W., Zhang, M., Vithanage, M., Mandal, S., Gao, B., Bolan, N.S., Ok, Y.S., 2016. Engineered/designer biochar for contaminant removal/immobilization from soil and water: potential and implication of biochar modification. *Chemosphere* 148, 276–291.
- Roco, C.A., Bergaust, L.L., Bakken, L.R., Yavitt, J.B., Shapleigh, J.P., 2017. Modularity of nitrogen-oxide reducing soil bacteria: linking phenotype to genotype. *Environmental Microbiology* 19, 2507–2519.
- Senbayram, M., Chen, R., Budai, A., Bakken, L., Dittert, K., 2012.  $\text{N}_2\text{O}$  emission and the  $\text{N}_2\text{O}/(\text{N}_2\text{O} + \text{N}_2)$  product ratio of denitrification as controlled by available carbon substrates and nitrate concentrations. *Agriculture, Ecosystems & Environment* 147, 4–12.
- Shen, J., Tang, H., Liu, J., Wang, C., Li, Y., Ge, T., Jones, D.L., Wu, J., 2014. Contrasting effects of straw and straw-derived biochar amendments on greenhouse gas emissions within double rice cropping systems. *Agriculture, Ecosystems & Environment* 188, 264–274.
- Šimek, M., Cooper, J.E., 2002. The influence of soil pH on denitrification: progress towards the understanding of this interaction over the last 50 years. *European Journal of Soil Science* 53, 345–354.
- Schmidt, C.S., Richardson, D.J., Baggs, E.M., 2011. Constraining the conditions conducive to dissimilatory nitrate reduction to ammonium in temperate arable soils. *Soil Biology and Biochemistry* 43, 1607–1611.
- Spott, O., Russow, R., Stange, C.F., 2011. Formation of hybrid  $\text{N}_2\text{O}$  and hybrid  $\text{N}_2$  due to codenitrification: first review of a barely considered process of microbially mediated N-nitrosation. *Soil Biology and Biochemistry* 43, 1995–2011.
- Van Zwielen, L., Singh, B.P., Kimber, S.W.L., Murphy, D.V., Macdonald, L.M., Rust, J., Morris, S., 2014. An incubation study investigating the mechanisms that impact  $\text{N}_2\text{O}$  flux from soil following biochar application. *Agriculture, Ecosystems & Environment* 191, 53–62.
- Verhoeven, E., Six, J., 2014. Biochar does not mitigate field-scale  $\text{N}_2\text{O}$  emissions in a Northern California vineyard: an assessment across two years. *Agriculture, Ecosystems & Environment* 191, 27–38.
- Wang, Z., Zheng, H., Luo, Y., Deng, X., Herbert, S., Xing, B., 2013. Characterization and influence of biochars on nitrous oxide emission from agricultural soil. *Environmental Pollution* 174, 289–296.
- Wankel, S.D., Ziebis, W., Buchwald, C., Charoenpong, C., de Beer, D., Dentinger, J., Xu, Z., Zengler, K., 2017. Evidence for fungal and chemodenitrification based  $\text{N}_2\text{O}$  flux from nitrogen impacted coastal sediments. *Nature Communications* 8, 15595.
- Wijler, J., Delwiche, C.C., 1954. Investigations on the denitrifying process in soil. *Plant and Soil* 5, 155–169.
- Xi, D., Bai, R., Zhang, L., Fang, Y., 2016. Contribution of anammox to nitrogen removal in two temperate forest soils. *Applied and Environmental Microbiology* 82, 4602–4612.
- Xu, R.K., Zhao, A.Z., Yuan, J.H., Jiang, J., 2012. pH buffering capacity of acid soils from tropical and subtropical regions of China as influenced by incorporation of crop straw biochars. *Journal of Soils and Sediments* 12, 494–502.
- Yanai, Y., Toyota, K., Okazaki, M., 2007. Effects of charcoal addition on  $\text{N}_2\text{O}$  emissions from soil resulting from rewetting air-dried soil in short-term laboratory experiments. *Soil Science & Plant Nutrition* 53, 181–188.
- Yao, Y., Gao, B., Zhang, M., Inyang, M., Zimmerman, A.R., 2012. Effect of biochar amendment on sorption and leaching of nitrate, ammonium, and phosphate in a sandy soil. *Chemosphere* 89, 1467–1471.
- Yuan, J.H., Xu, R.K., Zhang, H., 2011. The forms of alkalis in the biochar produced from crop residues at different temperatures. *Bioresource Technology* 102, 3488–3497.
- Zhang, J., Lan, T., Müller, C., Cai, Z., 2015. Dissimilatory nitrate reduction to ammonium (DNRA) plays an important role in soil nitrogen conservation in neutral and alkaline but not acidic rice soil. *Journal of Soils and Sediments* 15, 523–531.
- Zheng, J., Stewart, C.E., Cotrufo, M.F., 2012. Biochar and nitrogen fertilizer alters soil nitrogen dynamics and greenhouse gas fluxes from two temperate soils. *Journal of Environmental Quality* 41, 1361–1370.